

# Slow beams of massive molecules

S. Deachapunya<sup>1,2</sup>, P.J. Fagan<sup>3</sup>, A.G. Major<sup>1</sup>, E. Reiger<sup>4</sup>, H. Ritsch<sup>5</sup>, A. Stefanov<sup>1</sup>, H. Ulbricht<sup>1,a</sup>, and M. Arndt<sup>1</sup>

<sup>1</sup> Faculty of Physics, University of Vienna, Boltzmanngasse 5, 1090 Vienna, Austria

<sup>2</sup> Department of Physics, Faculty of Science, Burapha University, Chonburi 20131, Thailand

<sup>3</sup> R&D The DuPont Company, PO Box 80328, Experimental Station, Wilmington, DE 19880-0328, USA

<sup>4</sup> Kavli Institute of Nanoscience, TU Delft, Lorentzweg 1, 2628 CJ Delft, The Netherlands

<sup>5</sup> Institute of Theoretical Physics, University of Innsbruck, Technikerstraße 20, 6020 Innsbruck, Austria

Received 10 August 2007

Published online 24 October 2007 – © EDP Sciences, Società Italiana di Fisica, Springer-Verlag 2007

**Abstract.** Slow beams of neutral molecules are of great interest for a wide range of applications, from cold chemistry through precision measurements to tests of the foundations of quantum mechanics. We report on the quantitative observation of thermal beams of perfluorinated macromolecules with masses up to 6000 amu, reaching velocities down to 11 m/s. Such slow, heavy and neutral molecular beams are of importance for a new class of experiments in matter-wave interferometry and we also discuss the requirements for further manipulation and cooling schemes with molecules in this unprecedented mass range.

**PACS.** 39.10.+j Atomic and molecular beam sources and techniques – 33.80.Ps Optical cooling of molecules; trapping

## 1 Introduction

Stimulated by the great success of atom cooling and trapping experiments [1, 2], much effort has also been directed at demonstrating slow or cold molecular beams.

This includes the pioneering work on the deceleration [3] and trapping in electric [4, 5] or magnetic fields [6, 7]. Similarly the deceleration of the heavier YbF to 287 m/s was realized for new precision experiments [8]. Optical dipole forces were employed to slow C<sub>6</sub>H<sub>6</sub> to 300 m/s [9]. A back-rotating nozzle was used for reducing the speed of SF<sub>6</sub> to 55 m/s [10] and back-rotating silicon paddles significantly decelerated fast helium atoms [11]. Laser implantation into cryogenically cooled helium allowed the formation of PbO beams at 40 m/s [12]. The slowing of NO molecules in billiard-like collisions with Ar reduced their velocity to 15 m/s [13]. Slow and cold dimers were also formed in a reaction between counter-propagating H and halogen atoms [14]. Finally, cavity assisted optical manipulation methods [15] have recently been proposed for cooling external and internal [16] degrees of freedom in small molecules. The rapid evolution of molecule experiments opens the question if some of the new methods could also be applied to distinctively more massive systems. This is particularly interesting with regard to the stringent requirements of quantum interferometry with massive compounds [17].

Common to all such experiments is the need to volatilize complex materials at sufficiently low kinetic

energy, which is usually a great challenge. For organic molecules one often observes an increase in the particle's electric polarizability, dipole moment and number of weak bonds when the number of atoms per molecule is augmented. Correspondingly, there is an overall trend for large molecules to have a low vapor pressure and a high fragmentation probability at elevated temperatures.

Some of these problems can be circumvented by recurring to matrix assisted laser desorption (MALD) [20], jet expanded laser desorption (JETLD) [21] or electro-spray ionization (ESI) [22], but only at the expense of producing either fast (MALD, JETLD) or highly charged (ESI) molecular beams.

## 2 Experimental characterization of large molecules in the gas phase

In marked contrast to these observations, we here report on new perfluoroalkylated neutral particles in the mass range up to more than 6000 amu, whose vapor pressures are sufficiently high and whose velocities are sufficiently low to open a new experimental window for new coherent (interferometry, molecular lenses) or incoherent (cooling) molecular manipulation schemes.

### 2.1 Molecule

In particular we study the perfluoroalkylated carbon-sphere C<sub>60</sub>[(CF<sub>2</sub>)<sub>11</sub>CF<sub>3</sub>]<sub>n</sub>H<sub>m</sub>, where  $m \in \{0...2\}$  is the

<sup>a</sup> e-mail: hendrik.ulbricht@univie.ac.at

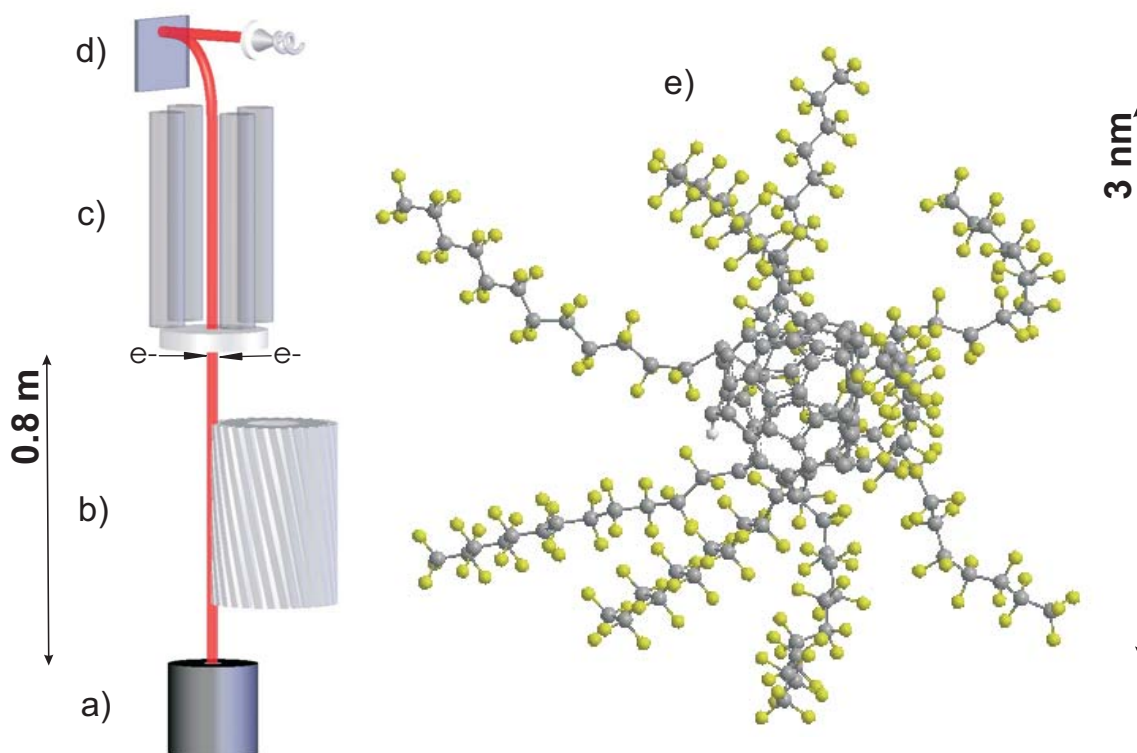


**Fig. 1.** (Color online) Setup for sublimation and velocity measurements: (a) thermal source (not to scale), (b) velocity selector, (c) electron impact ionization quadrupole mass filter and (d) detection unit. The structure of the perfluoroalkylated carbon sphere (e), also designated as perfluoro  $C_{60}$ .

number of attached H atoms and  $n \in \{0 \dots 9\}$  is the number of fluorinated side-chains attached to the  $C_{60}$  core. Figure 1 shows an energetically non-relaxed view of the molecule, to illustrate its overall structure and complexity. The molecules [23] were synthesized by one of the authors (P.F.). The mass of a nanosphere with  $n = 9$  side-chains exceeds that of any molecule in all previous slow-beam studies by more than an order of magnitude, and even that of a small protein, such as insulin ( $m \sim 5700$  amu).

## 2.2 Beam machine

Our experiments were performed in a vertical fountain configuration, which is crucial for measuring high intensities in particular for slow molecules, see Figure 1. The material was evaporated in a furnace with a circular aperture of  $500 \mu\text{m}$  diameter. The home-made helical velocity selector, shown in Figure 1 is located 5 mm above the furnace aperture and has a length of 140 mm and a radius of 48 mm. The velocity selection is done by channels (grooves) in the rim of the selector which have a slope with regard to the selector axis. The angle between the grooves and the rotor axis is 13 rad. The angular velocity of the rotor determines the mean velocity of the transmitted molecules. The bandwidth of  $\Delta v/v = 5\%$  (FWHM) is determined by the aspect ratio (width/length) of the

milled grooves in the selector. For our model, a rotation frequency of 1 Hz corresponds to a molecule velocity of 1.08 m/s and the mean transmitted velocity scales linearly with the rotor frequency. The phase stability of the rotation of the selector was carefully checked and maintained with a stroboscopic flash lamp operating at the rotation frequency with  $\Delta f = 0.1\%$ . Having passed the selector, and after a drift region of 0.5 m above the furnace the perfluorinated compounds were finally detected using electron impact ionization quadrupole mass spectroscopy in a differentially pumped second vacuum chamber. We used an Extrel quadrupole mass spectrometer with electron energy of  $E_{kin} = 40 \dots 70$  eV which allows to detect molecules with masses up to 9000 amu. We here report on the first electron impact ionization for detecting those large perfluoroalkylated molecules [23]. For the mass spectrum shown in Figure 2a the spectrometer was optimized to the signal of nanospheres with  $n = 7$  side-chains (see discussion below).

## 2.3 Characterization of the carbon nanospheres

Figure 2a shows a mass spectrum of the post-ionized perfluoroalkylated carbon spheres. We identify molecules with between one and nine intact side chains. The relative intensity of these peaks is determined by the chemical

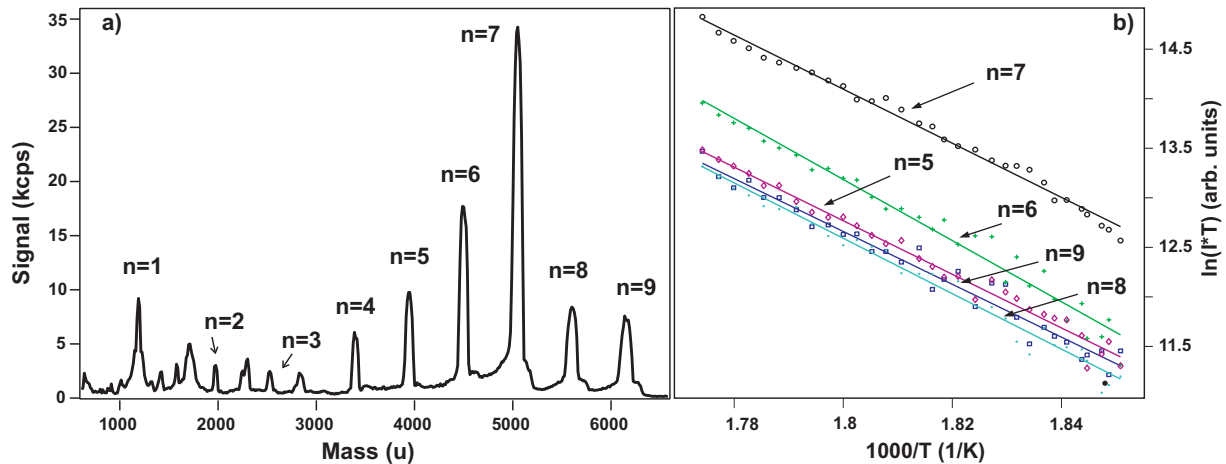


**Fig. 2.** (Color online) Panel (a) shows a typical mass spectrum of perfluoro  $C_{60}$  at 545 K. The integer  $n$  counts the number of perfluoroalkylated side-chains attached to the central buckyball. The mass spectrometer parameter are optimized for most efficient detection of the  $n = 7$  compound. Panel (b) is the Arrhenius plot to evaluate the sublimation enthalpy for  $n = 5 \dots 9$  compounds.

**Table 1.** Sublimation enthalpies for large perfluoroalkyl-functionalized molecules: the temperature interval for the sublimation studies ( $T_m$ ) and the experimental decomposition temperature ( $T_d$ ) were  $T_m = 540\text{--}563$  K and  $T_d = 650$  K. Error bars are evaluated from curve fitting deviations.

Molecule	Mass (u)	$\Delta H_{sub}$ [kJ/mol]
Perfluoro $C_{60}$ , $n = 9$	6291	$217 \pm 15$
Perfluoro $C_{60}$ , $n = 8$	5672	$227 \pm 13$
Perfluoro $C_{60}$ , $n = 7$	5053	$222 \pm 8$
Perfluoro $C_{60}$ , $n = 6$	4434	$251 \pm 16$
Perfluoro $C_{60}$ , $n = 5$	3815	$220 \pm 11$

synthesis and might be influenced by the chemical rearrangements during long-time storage, spectrometer settings as well as fragmentation processes during both the evaporation and the ionization process. But the variation of their peak height with the furnace temperature is an absolute measure for their sublimation enthalpy. In order to quantify this, we linearly ramp the temperature with a heating rate of 0.7 K/min and record the exponential increase of the count rate. Using the Clausius-Clapeyron equation we evaluate the sublimation enthalpy  $\Delta H_{sub}$  from an Arrhenius fit to the data (see Fig. 2b). The results are summarized in Table 1.

We have also estimated the scalar polarizability  $\alpha$  using the software Gaussian 03 [24] with a reduced Hartree-Fock method and the 6-31 G polar basis. We find a scalar static polarizability of  $\alpha = 194 \text{ \AA}^3$  and a permanent dipole moment of about 6 Debye for the carbon nanosphere with  $n = 7$ . The compound with  $n = 1$  was calculated to have a static polarizability of  $\alpha = 84 \text{ \AA}^3$  which is close to the measured value for an individual  $C_{60}$  molecule [35]. Each additional side-chain adds to the total polarizability with about  $18 \text{ \AA}^3$ . The low  $\alpha/m$ -value is consistent with the unusually high vapor pressure of these perfluorinated compounds, making them particularly useful for generating slow thermal beams.

All sublimation enthalpies are equal within their error bars. This is both compatible with an possible initial mixture of different perfluoroalkylated carbonspheres with very similar  $\alpha/m$  ratios, as well as with a monodisperse distribution of large molecules, undergoing fragmentation in the ionization process. The compound of the perfluoro  $C_{60}$  with seven side chains had the highest absolute signal in this series of experiments. It reached up to 750 000 cps at 635 K, corresponding to a molecular flux of  $10^{11} \text{ s}^{-1} \text{ cm}^{-2}$  in the detection region — that is 800 mm above the furnace. From the measured flux and the velocity we can calculate the number density to be  $10^{13} \text{ cm}^{-3}$  for a distance 3 mm above the source exit (see cavity focusing below). Here we assume a rather conservative total detection efficiency for the neutral particles of about  $\eta = 10^{-4}$ . This estimate is based on the observation by Bart et al. [25] that the electron impact ionization cross section per bond can be extrapolated to larger perfluorinated hydrocarbons. The electron impact ionization cross section here was thus estimated to be  $\sigma_{\text{perfluoro } C_{60}} = 2.7 \times 10^{-18} \text{ m}^2$ .

The observation of a rather high flux of intact neutral and very massive molecules is a key result of great importance for the proposed interferometry and optical manipulation applications.

## 2.4 Velocity measurements

Earlier experiments already showed that matter wave interferometry is well feasible for de Broglie wavelengths larger than about one picometer [17]. For molecules with a mass of 5000 amu this limit is touched at a velocity of 55 m/s. Help in this situation may come from the expectation that massive molecules from thermal sources propagate at low mean velocities. We therefore present in Figure 3 the velocity spectrum of the carbon nanospheres with  $n = 7$  side chains. We observed a floating Maxwell-Boltzmann distribution

$$f(v) = v^2 \exp\left(-\frac{m(v - v_m)^2}{2k_B T}\right), \quad (1)$$

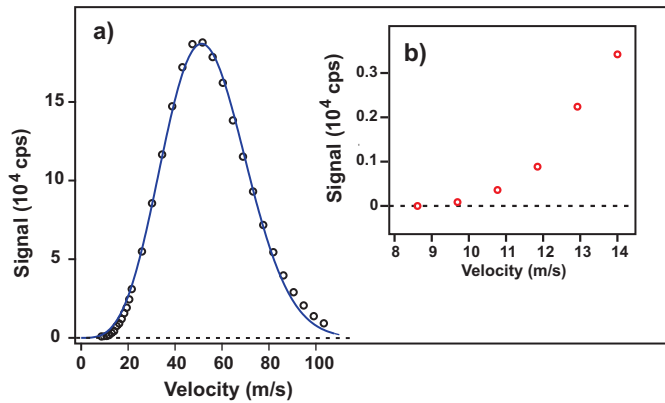


**Fig. 3.** (a) Velocity distribution of the isomer  $n = 7$  ( $m = 5053$  amu) of the perfluoroalkylated carbon nanosphere at 585 K. The solid line represents a fit with a floating Maxwell-Boltzmann distribution. (b) The inset shows molecules even at velocities down to 11 m/s.

with a most probable velocity of  $v_m = 51$  m/s, which is about 15% faster than  $v_m = \sqrt{2k_B T/m} = 44$  m/s, which would be expected for a fully effusive beam. The width of the curve fits to an ensemble temperature of 302 K, compared to the source temperature of 585 K. This indicates that the source operates at the transition between an effusive and a weakly supersonic beam [26] which provides already translational cooling by a factor of two. But even more importantly, we still find a detectable fraction of particles at velocities down to 11 m/s. Such low velocities may come as a surprise, given the well-established fact that in atomic fountains the slow fraction of the atomic ensemble is usually suppressed by collisions with faster particles [37].

Although while we also see a shift to higher velocities, we still maintain an overall slow envelope, since our seed gas is the molecule itself with a mass of about 5000 amu and the experimental observation is in good agreement with elementary theoretical expectations.

The rather significant signal at low velocities is very promising for testing matter-wave physics in an unprecedented mass range using a new interferometer concept that has recently been developed in our group [27]. With regard to future matter wave experiments it is important to see, that the geometrical cross section of perfluoroalkylated particles exceeds that of  $C_{60}$  already by a factor of about ten, while their scattering cross section, determined by the van der Waals interaction, remains still comparable. This is particularly relevant with respect to the suppression of collisional decoherence [28].

### 3 Optical manipulation of massive molecular beams

Given the low velocity of these heavy molecules it is intriguing to also explore the possibilities for new post-processing schemes to reshape and possibly further increase the phase-space density using off-resonant light

fields. We start by first estimating the laser power which is required to manipulate molecules with a thermal kinetic energy of  $\sim 50$  meV. This corresponds to a velocity of 44 m/s for the  $n = 7$  perfluoroalkylated nanosphere. A far-detuned Gaussian laser beam of power  $P$ , focused to a waist of  $w_0 = 100 \mu\text{m}$ , creates a dipole potential of well-depth

$$U = \frac{2\alpha P}{(\varepsilon_0 c \pi w_0^2)}, \quad (2)$$

i.e. of 3.3 neV per Watt for a molecular polarizability of  $200 \text{ \AA}^3$ . A power of  $P = 15$  MW is therefore needed, if we wish to fully compensate the kinetic energy of our supermassive molecules. This power can be provided by a common Q-switched laser with a pulse energy of 75 mJ delivered in a pulse duration of 5 ns. However, we also have to consider that about  $N_{abs}$  photons are absorbed by each molecule during the interaction time  $\tau$  with the laser, where

$$N_{abs} = \frac{I_0 \sigma \tau}{(h\nu)} = \frac{2P\sigma\tau}{(\pi w_0^2 h\nu)}. \quad (3)$$

Since our perfluorinated compounds have an NIR (1064 nm) absorption cross section of  $\sigma_{1064} = 3 \times 10^{-23} \text{ m}^2$ , a 75 mJ stopping laser would deposit about 770 photons in each molecule and would thus be likely to destroy the particle. The  $\sigma$ -value was measured for solvated molecules and it might be smaller by an order of magnitude for molecules in the gas-phase [29].

Higher intensities can be achieved with shorter laser pulses: let us consider a picosecond laser with a pulse duration of 7.5 ps, a pulse energy of 3 mJ, a wavelength of 1064 nm, and a waist of 1 mm, which is counter-propagating with respect to the molecular beam (see Fig. 4c). It would generate an off-resonant slowing/focusing potential of 13 meV in both the transverse and the longitudinal molecular beam direction. A fraction of the molecules will be decelerated by about 6 m/s. Only 0.3 IR photons would be absorbed by each molecule per light pulse. Slowing of our molecules by pulsed laser light will therefore work as good as reported before for benzene molecules [9].

#### 3.1 Optical focusing in a cavity

It might be of even greater relevance not to stop a pulsed molecular beam but rather to transversely guide and colimate a subset of continuously emerging molecules. Here we are aiming at an increased signal for interference and spectroscopy experiments. As a first example, we consider realizing an optical lens for these molecules by passing them through a focused Gaussian mode of an intense laser beam. Using a high-Q build-up cavity, intra-cavity intensities of up to  $10^4$  W are well conceivable, which, focused to a waist of  $100 \mu\text{m}$ , would provide an optical potential depth of 0.03 meV. For  $m = 5053$  amu we see that the transverse potential would capture all molecules with

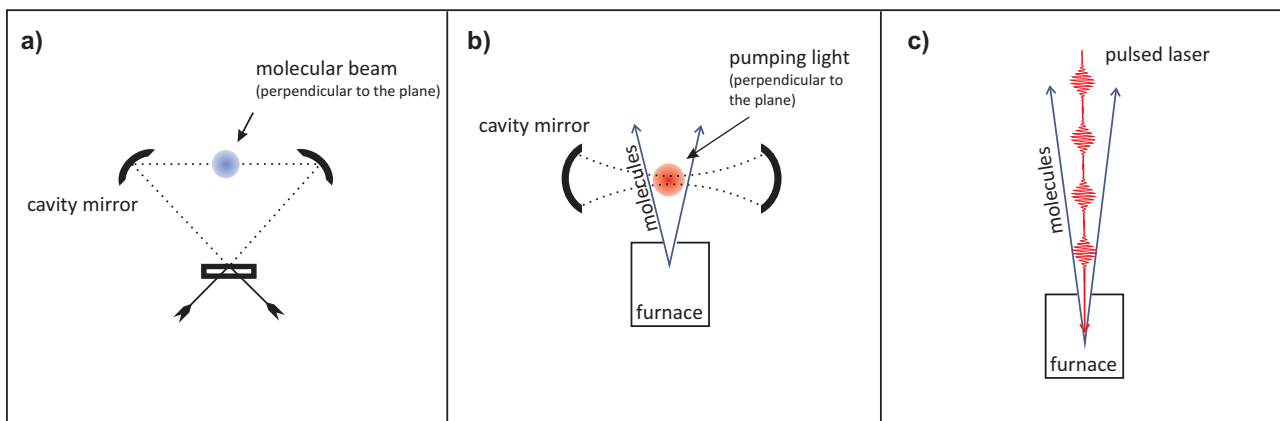


**Fig. 4.** Discussed setups: a ring-cavity for optical focusing/collimation (a) and a linear cavity for optical cooling (b) of molecules, generated from a thermal source. The pump laser beam is perpendicular to both the axis of the cavity and the direction of the molecular beam for the linear cavity. Only the light scattered by the molecules couples into the cavity. Panel (c) is a setup for molecular beam slowing with counter-propagating pulsed laser light.

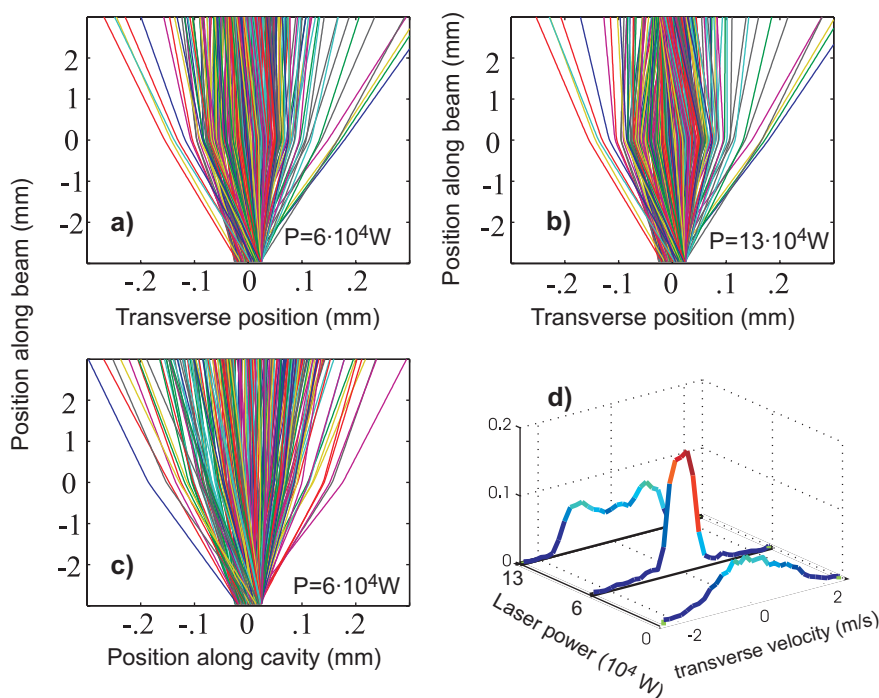


**Fig. 5.** (Color online) Numerical simulation of transverse optical focusing of a molecular beam in a build-up ring cavity focused at the origin of our coordinate system, 3 mm above the source exit. Panels (a) and (b) show focusing transverse to the laser and molecular beam for two different intra-cavity laser powers, while panel (c) shows the motion along the laser beam. In panel (d) we show the final molecular velocity distributions after transit of the field for three different intra-cavity powers.

a transverse speed of up to 1 m/s. Hence, such a cavity enhanced laser beam close to the oven, should increase the molecular flux at the position of the detector. Each molecule would absorb about 200 IR photons (1064 nm) during the passage through the focusing cavity which should be close to the damage threshold.

To illustrate a realistic scenario we simulate the collimation of a beam of 5000 amu particles in a cavity enhanced laser field of  $6 \times 10^4 \text{ W}$ . The perturbing influence of a standing light wave force grating would be eliminated in a ring cavity (see Fig. 4a). The proposed collimation cavity is very similar in dimensions to one used to optically trap  $^{85}\text{Rb}$  atoms [31]. In Figure 5 we show simulated trajectories of molecules with an average velocity of  $\bar{v} = 50 \text{ m/s}$  and a transverse and longitudinal veloc-

ity spread of  $\pm 1 \text{ m/s}$  emanating from a square shaped source of  $50 \times 50 \mu\text{m}^2$ . This is the fraction of molecules which are captured and focused by a Gaussian beam of  $w_0 = 100 \mu\text{m}$  and Rayleigh length of  $z_R \sim 3 \text{ cm}$ , positioned at  $d = 3 \text{ mm}$  above the opening of the thermal source. For a properly chosen intensity, collimation and/or focusing can be achieved in both transverse directions at input laser powers in the 1...10 W range.

We therefore expect a signal gain in the forward direction by about a factor of two, when using a single cavity and up to a factor of four, when using two orthogonal fields. This increase is already rather significant and will enable interferometry experiments with these larger perfluoroalkylated molecules [36].



### 3.2 Optical cooling in a cavity

In an experimentally more challenging next step one can employ cavity mediated laser cooling of these macromolecular beams. As individual particles are only very weakly coupled to the light field, standard cavity cooling [30,32] is too slow to be useful without an additional trap, but the use of collective effects will yield a measurable result. Here we suggest a linear confocal cavity with the axis perpendicular to both the direction of the molecular beam and the pumping light (see Fig. 4b). For a 1 cm long cavity with a 400  $\mu\text{m}$  waist and a line width of  $\kappa \approx 2\pi \times 1$  MHz at 1 mm above the source one would expect cooling times of seconds for individual molecules. However, given the high number density of  $N > 10^9$  perfluorinated particles in the cavity mode volume of 1.2  $\text{mm}^3$ , close to the furnace exit, one can expect a substantial collective enhancement of the cooling effect. Additional light scattering at intra-cavity molecules in the direction of the mode further deepens the cooling potential and enhances cooling in the direction of the cavity. The cavity photon number and therefore the enhancement effect scales with  $N^2$  [33]. Efficient cooling in a single mode can be achieved as soon as the self-organization threshold light power  $P_T = 1 \times 10^3$  W is reached [34]. As an example, we calculate the single mode energy loss and the associated change of the transverse velocity distribution of perfluorinated molecules propagating perpendicular to the cavity axis with the slowest experimentally observed velocity in Figure 6. Using two modes of the same cavity (or two cavities) the required pump threshold corresponds to about one Watt of input power for a cavity with a finesse  $F \approx 10^3$ .

## 4 Conclusion

In conclusion, we have demonstrated that even very massive molecules can form very slow beams at useful intensities. They are very promising for future matter-wave experiments and appear to be accessible for a number of optical slowing and cooling experiments with molecules in a new mass regime. Furthermore the exploration of cryogenic cooling schemes could be interesting with these molecules. The doping of perfluoroalkylated nanospheres into cold helium nanodroplets would possibly be a method for enabling high resolution spectroscopy on rather complex molecules [38].

This work was supported by the Austrian Science Funds FWF through START Y177, SFB F1505 and F1512, and a Lise-Meitner fellowship (A.G.M.). We acknowledge support by the European Commission (HPRN-CT-2002-00309 for E.R. and A.S.) and by the Royal Thai government scholarship (S.D.). We thank William Case for fruitful discussions.

## References

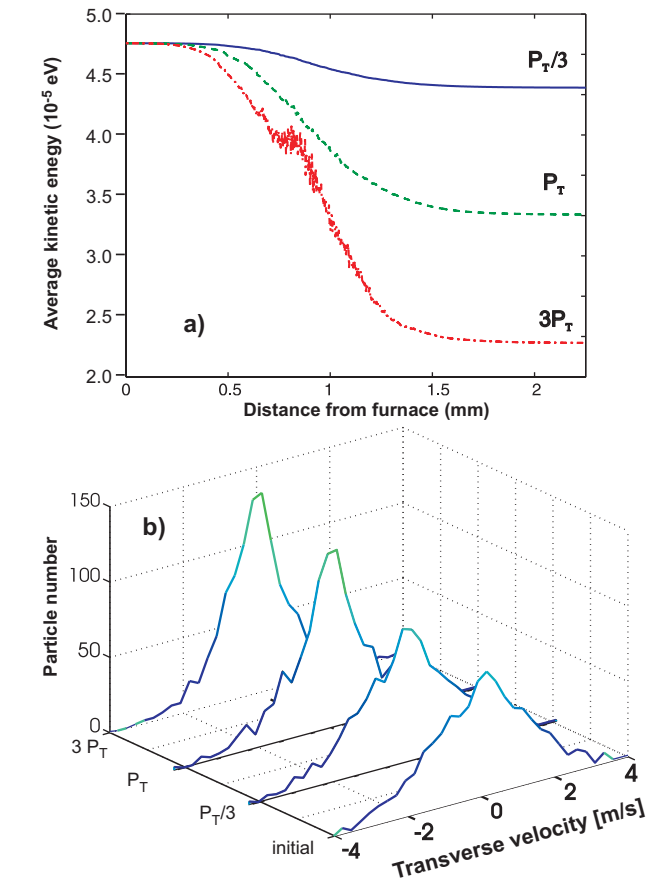


**Fig. 6.** Cavity assisted optical cooling in one transverse molecular beam direction: (a) time evolution of kinetic energy along cavity axis for  $N = 1000$  particles of mass 5000 amu, passing through a cavity with waist  $w_0 = 400 \mu\text{m}$  with average velocity of 10 m/s ( $\Delta v = 1.5$  m/s) for different laser powers  $P = P_T/3, P_T, 3P_T$ , where  $P_T = 1$  kW is the effective self-organization threshold, (b) initial and final transverse velocity distributions for these parameters. Note that we rescaled the interaction strength to mimic the actually higher molecule density from the source.

2. *Interactions in ultracold gases*, edited by M. Weidemüller, C. Zimmermann (Wiley-VCH, 2003)
3. H.L. Bethlem, G. Berden, F.M.H. Crompvoets, A.J.A. van Roij, R.T. Jongma, G. Meijer, *Nature* **406**, 491 (2000)
4. F.M.H. Crompvoets, H.B.R. Jongma, G. Meijer, *Nature* **411**, 174 (2001)
5. T. Junglen, T. Rieger, S. Rangwala, P. Pinkse, G. Rempe, *Eur. Phys. J. D* **31**, 365 (2004)
6. J.M. Doyle, B. Friedrich, J. Kim, D. Patterson, *Phys. Rev. A* **52**, R2515 (1995)
7. B.C. Sawyer, B. Lev, E.R. Hudson, B.K. Stuhl, M. Lara, J.L. Bohn, J. Ye, e-print [arXiv:physics/0702146v1](https://arxiv.org/abs/physics/0702146v1)
8. M.R. Tarbutt, H.L. Bethlem, J.J. Hudson, V.L. Ryabov, V.L. Ryzhov, B.E. Sauer, G. Meijer, E.A. Hinds, *Phys. Rev. Lett.* **92**, 173002 (2004)
9. R. Fulton, A.I. Bishop, P.F. Barker, *Phys. Rev. Lett.* **93**, 243004 (2004)
10. M. Gupta, D. Herschbach, *J. Phys. Chem. A* **105**, 1626 (2001)

11. E. Narevicius, A. Libson, M.F. Riedel, C.G. Parthey, I. Chavez, U. Even, M.G. Raizen, *Phys. Rev. Lett.* **98**, 103201 (2007)
12. S.E. Maxwell, N. Brahms, R. deCarvalho, J. Helton, S. Nguyen, D. Patterson, D. Glenn, J. Petricka, D. DeMille, J.M. Doyle, *Phys. Rev. Lett.* **95**, 173201 (2005)
13. M.S. Elioff, J.J. Valentini, D.W. Chandler, *Science* **302**, 1940 (2003)
14. N.N. Liu, H. Loesch, *Phys. Rev. Lett.* **98**, 103002 (2007)
15. P. Horak, G. Hechenblaikner, K.M. Gheri, H. Stecher, H. Ritsch, *Phys. Rev. Lett.* **79**, 4974 (1997)
16. G. Morigi, P.W.H. Pinkse, M. Kowalewski, R. de Vivie-Riedle, e-print [arXiv:quant-ph/0703157v1](https://arxiv.org/abs/quant-ph/0703157v1)
17. M. Arndt, O. Nairz, J. Voss-Andreae, C. Keller, G.V. der Zouw, A. Zeilinger, *Nature* **401**, 680 (1999)
18. O. Nairz, B. Brezger, M. Arndt, A. Zeilinger, *Phys. Rev. Lett.* **87**, 160401 (2001)
19. B. Brezger, L. Hackermüller, S. Uttenthaler, J. Petschinka, M. Arndt, A. Zeilinger, *Phys. Rev. Lett.* **88**, 100404 (2002)
20. K. Tanaka, H. Waki, Y. Ido, S. Akita, Y. Yoshida, T. Yoshida, T. Matsuo, *Rap. Comm. Mass Spectr.* **2**, 151 (1988)
21. J. Grotemeyer, U. Boesl, K. Walter, E.W. Schlag, *OMS* **21**, 645 (1986)
22. J.B. Fenn, M. Mann, C.K. Meng, S.F. Wong, C.M. Whitehouse, *Science* **246**, 64 (1989)
23. P.J. Fagan, P.J. Krusic, C.N. McEwen, J. Lazar, D. Holmes Parkert, N. Herron, E. Wasserman, *Science* **262**, 404 (1993)
24. M.J. Frisch, G.W. Trucks, H.B. Hudson, G.E. Scuseria, *GAUSSIAN03* (Revision A. 11.4), 2002
25. M. Barth, P.W. Harland, J.E. Hudson, C. Vallance, *Phys. Chem. Chem. Phys.* **3**, 800 (2001)
26. *Atomic and Molecular Beam Methods*, edited by G. Scoles, D. Bassi, U. Buck, D. Lainé (University Press, Oxford, 1988)
27. S. Gerlich, L. Hackermüller, K. Hornberger, A. Stibor, H. Ulbricht, M. Gring, F. Goldfab, T. Savas, M. Müri, M. Mayor, M. Arndt, *Nature Phys.* **3**, 711 (2007)
28. K. Hornberger, S. Uttenthaler, B. Brezger, L. Hackermüller, M. Arndt, A. Zeilinger, *Phys. Rev. Lett.* **90**, 160401 (2003)
29. N. Gotsche, H. Ulbricht, M. Arndt, *Laser Phys.* **17**, 583 (2007)
30. P. Maunz, T. Puppe, I. Schuster, N. Syassen, P.W.H. Pinkse, G. Rempe, *Nature* **428**, 50 (2004)
31. D. Kruse, M. Ruder, J. Benhelm, C. von Cube, C. Zimmermann, P.W. Courteille, T. Elsässer, B. Nagorny, A. Hemmerich, *Phys. Rev. A* **67**, 051802(R) (2003)
32. P. Domokos, P. Horak, H. Ritsch, *J. Phys. B: At. Mol. Opt. Phys.* **34**, 187 (2001)
33. P. Domokos, H. Ritsch, *Phys. Rev. Lett.* **89**, 253003 (2002)
34. J.K. Asboth, P. Domokos, H. Ritsch, A. Vukics, *Phys. Rev. A* **72**, 053417 (2005)
35. M. Berninger, A. Stefanov, S. Deachapunya, M. Arndt, *Phys. Rev. A* **76**, 013607 (2007)
36. S. Deachapunya, A. Stefanov, M. Berninger, H. Ulbricht, E. Reiger, N. Doltsinis, M. Arndt, *J. Chem. Phys.* **126**, 164304 (2007)
37. N. Ramsey, *Rev. Mod. Phys.* **62**, 541 (1990)
38. F. Stienkemeier, K.K. Lehmann, *J. Phys. B* **39**, R127 (2006)